Analyst

Accepted Manuscript

ROYAL SOCIETY OF CHEMISTRY

www.rsc.org/analyst

Journal Name

COMMUNICATION

Analysis of the Lipid Profiles in Sectional Bovine Brain via Non-Catalytic Rapid Methylation

Received 00th January 20xx,
Accepted 00th January 20xx

DOI: 10.1039/x0xx00000x

www.rsc.org/

Jong-Min Jung[a], Ki-Hyun Kim[b], Eilhann E. Kwon[a*], and Hyung-Wook Kim[c*]

The main focus of this study is to mechanistically introduce a new-fashioned qualitative and quantitative technique for mapping the lipid profile of a sectional brain via non-catalytic transesterification reaction (*i.e.,* pseudo catalytic reaction in the presence of porous materials). One of the biggest technical advances achieved in this study is the qualitative and quantitative analysis of lipid from bovine brain at trace quantities in the magnitude of μg via the non-catalytic pathway. Moreover, newly introduced derivatization in this work showed high tolerance against impurities (*i.e.,* water and extractives)

Introduction

Triglyceride has been known to be one of the most common chemical compounds in all living organisms[1]. It plays essential roles associated with cellular structure and organization, signal transduction, protein regulation, metabolic transformation and cellular trafficking[2-4]. Therefore, a new-fashioned inspired area of research called lipidomics has been actively proposed to mechanistically investigate the in-depth knowledge covering various biological metabolic phenomena and pathological cases[5-7].

Especially in the field of medicine/neuroscience, the precise lipid analysis could be powerful tools that could be applicable to various purposes. For instance, molecular and structural changes triggered by dysregulated lipids in neuronal synapses have been identified through the numerous long-standing studies[2, 8-11]. Similarly, many researchers reported unexpected alternation of lipid profiles in patient's brains suffering from various neurodegenerative and neuropsychiatric diseases, which was partially confirmed by the significant synaptic loss and dysfunction in postmortem brains [8]. In addition to alteration of the lipid profiles, neuronal membrane instabilities have also been reported by many pathological case studies: a great deal of studies have reported pathological cases showing lower total phospholipids in the frontal cortex, a lower plasmenylethanolamine concentration and higher phosphatidylserine concentration in postmortem brains with Alzheimer's disease (AD): a substantial reduction in the total amount of n-3 polyunsaturated fatty acid (PUFA) and docosahexaenoic acid (DHA, 22:6n-3) was observed in the postmortem brain and in the plasma of AD patients[7, 12]. Furthermore, several studies have identified a substantial reduction of DHA in the postmortem brain and in the plasma of patients with bipolar disorder (BPD), a major neuropsychiatric disorder[5, 9, 13-15].

Our demand for the precise technique for the lipid profiles of the brain as a biomarker and as a powerful diagnostic tool enabling us to trace the lipid profiles in plasma and/or in brains impaired by various acute and/or chronicle diseases has been fully recognized by the research communities[5, 7]. Unfortunately, the practical and reliable adaptation for the analysis of the precise lipid profiles as a diagnostic indicator has not been fully implemented due to the technical limitations arising from different methodologies, analysed brain regions, tissue quality, sample size, and so on.

The most common lipid profiling of brains has been conducted via the derivatizing triglycerides (TGs) and phospholipids into fatty acid methyl esters (FAMEs)[16-27]. This derivatization is routinely conducted via the transesterification reaction under the presence of the homogeneous catalysts (*i.e.,* KOH/NaOH/H_2SO_4) at temperatures of 60-63 ˚C, which has been known to be very sensitive to impurities such as

[a] *Department of Environment & Energy, Sejong University, Seoul 143-747, South Korea*
[b] *Department of Civil and Environmental Engineering, Hanyang University, Seoul 133-791, South Korea*
[c] *Department of Biological Science and Technology at Sejong University, Seoul 143-747, South Korea*

† Footnotes relating to the title and/or authors should appear here. Electronic Supplementary Information (ESI) available: [details of any supplementary information available should be included here]. See DOI: 10.1039/x0xx00000x

water and various extractives[28]. Thus, the hierarchical pretreatment steps for the purification of lipids with a thin layer chromatography (TLC) must be followed[29, 30]. These purification steps have been known to be very time consuming and are considered to be the crucial factor for loss of TGs and phospholipids. In addition, the stated technical limitations have implied that the whole spectrum of the lipid profiles would be very challenging since perfect purification could not be expected. Thus, new technical advances for derivatizing lipids into FAMEs should be established.

The main goals of this work are to provide and validate new technical methods for the simultaneous derivatization of TGs and phospholipids into FAMEs without the purification steps (*i.e.,* direct derivatization after solvent extraction of brain). In addition, another objective of this work is to qualitatively and quantitatively acquire the lipid profiles of sectional brain in light of the unavailability of region-specific information on lipid compositions. As a case study, the lipid profiles of the six dissected bovine brains were transformed into FAMEs via the non-catalytic pathway via using a porous material. A great deal of studies covering lipid analysis has been well archived, but the derivatization of lipid into FAMEs with porous material has been unprecedented. Therefore, this work provides not only the mechanistic explanation and validation of new derivatizing techniques using porous material but also whole spectrum of lipid profiles for the region-specific information on dissected bovine brain.

2. MATERIALS AND METHOD

2.1. Reagents and Preparation

Bovine brain was purchased from a local market, which collected it based on the Korean Ministry of Agriculture, Food, and Rural Affairs (MAFRA) animal use and care protocols. Refined sunflower seed oil was purchased from a local market. The brain tissues were dissected based on the bovine brain atlas and then frozen at a temperature of -80 ˚C until use. Anhydrous methanol (Lot: 322415, CAS Number 67-56-1, MW: 32.04), sulfuric acid (Lot: 339741, CAS Number 7664-93-9, MW: 98.08), NaOH (Lot: 221465, CAS Number 1310-73-2, MW: 40.00), and anhydrous n-hexane (Lot: 296090, CAS Number 110-54-3, MW: 86.15) were purchased from Sigma Aldrich (St. Louis, USA). Silica with an average pore diameter of 60 Å (Lot: 236799-100G, 60-100 mesh) and 150 Å (Lot: 236810-100G, 200-425 mesh) was purchased from Sigma Aldrich (St. Louis, USA). The porous material was dried at 80 ˚C for 72 h and then stored in a desiccator. Lipid extraction of six dissected bovine brain tissues was conducted with a Soxhlet unit at 90 ˚C for 10 h and then solvent was recovered by using a rotary evaporator (Thermo Scientific, USA).

2.2. Conventional Transesterification

In order to transesterify sunflower seed oil, 1 M NaOH was attained through dissolution into MeOH. An equivolume mixture of sunflower seed oil and MeOH was placed in 200 mL flask and connected to a reflux condenser with water circulation. A 100 mL of mixture solution was heated at 60 ˚C with stirring at 300 rpm (2 h). Replicate analysis was conducted with the extracted lipid (from six dissected bovine brains) with sulfuric acid (instead of NaOH). All experimental conditions for the transesterification reaction were maintained identically except for the reaction time. Extracted lipid was transesterified for 48 h.

2.3. Transesterification under the Presence of Porous Material

0.25 inch of a bulkhead unit (part number: SS-400-61) was purchased from Swagelok (USA) to use as a batch-type tubular reactor (TR) in this study. The equivolume ratio between the extracted lipid and MeOH was maintained as explained in Sec. 2.2. Next, 200 µL of this mixture was injected into the bulkhead, and 0.3 g of silica was inserted subsequently. The other side of the bulkhead was then capped and placed in the muffle furnace for 6 min. After that, the sealed bulkhead was chilled with 4 ˚C of water. In order to ensure the reproducibility, the experimental work based on each text matrix was repeated three times. The converted FAMEs were collected with organic solvent (*i.e.,* dichloromethane).

2.4. Chemical Analysis

Table 1. Calibration information on the target compounds

Order	Compounds	MW (g mol^{-1})	Formula	ChemSpider ID	T_R (min)	RF (1/ng)	R^2
1	Methyl Cis-9-Oleate	296.49	C18:1	4516661	20.78	480.72	0.9999
2	Methyl Stearate	298.50	C18:0	7909	20.46	460.06	0.9998
3	Methyl Pamitate	270.45	C16:0	23255829	17.43	499.79	0.9999
4	Methyl Nervonate	380.65	C24:1	4516967	31.40	399.12	0.9991
5	Methyl cis-11-Eicosanoate	324.54	C20:1	4575789	24.74	438.40	0.9998
6	Methyl Lignocerate	382.66	C24:0	68071	31.15	309.99	0.9993
7	Methyl Erucate	352.59	C22:1	4516577	28.29	422.16	0.9998
8	Methyl Palmitoleate	268.43	C16:1	558899	17.67	491.05	0.9997
9	Methyl Behenate	354.61	C22:0	12995	28.05	429.93	0.9997
10	Methyl Tricosanoacte	368.64	C23:0	68045	29.62	405.48	0.9999
11	Methyl Heptadecanoate	284.48	C17:0	14849	18.73	398.22	0.9999
12	Methyl Linolenate(Cis)	292.46	C18:3	4477947	22.86	480.48	0.9999
13	Myristoleic Acid Methyl Ester	240.38	C14:1	4509536	15.68	506.60	0.9999
14	Methyl Cis-10-Pentadecanoate	254.41	C15:1	21988	16.67	506.60	0.9999
15	Methyl Arachidate	326.56	C20:0	13621	24.49	438.28	0.9999
16	Methyl Pentadecanoate	256.42	C15:0	21988	16.32	499.79	0.9999
17	Methyl Linoleate	294.47	C18:2	4447491	21.68	441.56	0.9999
18	Methyl Myristate	242.40	C14:0	29024	15.37	523.58	0.9999
19	Methyl Cis-13,16-Docosadienoate	350.58	C22:2	21169417	29.03	480.51	0.9803

Journal Name

COMMUNICATION

Dilution of the extracted sample (*i.e.,* 1:15) was carried out prior to the direct injection analysis by GC/FID (Varian 450 High Resolution Gas Chromatograph) equipped with DB-Wax column (Agilent J&W GC column, 30 m×0.25 mm×0.25 μm). All operational GC parameters are summarized in Table SI-1 (*i.e.,* Supplementary Information). Multiple calibrations were conducted with FAME standard (37 FAME MIX, CRM47885, Sigma Aldrich, St. Louis, USA) as summarized in Table 1. The MDL values of 19 target compounds averaged as 0.57±0.29 ng (per 1 μL injection). Refer to Table SI-3 for detailed information regarding the basic QA parameters derived from the calibration analysis (*e.g.,* MDL and RSE). For the identification of each individual of all target FAMEs, replicate samples were also analyzed by GC/TOF-MS (Agilent 7890B/ALMSCO BENCH TOF) with the same operational parameters used for the GC/FID analysis.

3. RESULT AND DISUSSIONS

3.1. Heterogeneous Reaction in the Presence of Porous Material

FAMEs can be derivatized via transesterifying TGs in the presence of alkali/acid catalyst. There are three stepwise reactions with intermediate formation of diglyceride (DG) and monoglycerides (MG) yielding 3 moles of methyl ester (ME) as follows[28].

The overall catalytic reaction pathways can be summarized as:

$$TG + 3ROH \xrightarrow{CATALYST} 3R^{'}CO_2R + GL$$

The stepwise reactions are:

$$TG + ROH \underset{k_4}{\overset{k_1}{\rightleftharpoons}} DG + R^{'}CO_2R \quad (E_a = 14.7 kcal/mol)$$

$$DG + ROH \underset{k_5}{\overset{k_2}{\rightleftharpoons}} MG + R^{'}CO_2R \quad (E_a = 14.2 kcal/mol)$$

$$MG + ROH \underset{k_6}{\overset{k_3}{\rightleftharpoons}} GL + R^{'}CO_2R \quad (E_a = 6.4 kcal/mol)$$

The reaction rate constant denoted as k in the equations above is proportional to the temperatures and the order of magnitude of k has been known as *kMG>kDG>kTG*. One important thing to note in the above equations is that the activation energies for the stepwise reaction are relatively lower than those of other catalytic applications: total activation energies initiating the transesterification reaction are substantially lower than those in other catalytic applications (*i.e.,* 5.4% of those in the methane steam reforming process). Thus, non-catalytic transesterification has been achieved under the supercritical conditions (*i.e.,* 200-450 ˚C and 250-450 bar)[28]. Despite the numerous technical advantages, the practical implementation has been impeded due to the challenging operational parameters (*i.e.,* 200-450 ˚C and 250-450 bar), high capital cost, and safety issues.

However, our previous work[16, 31, 32] reported not only that the main driving force initiating the transesterification reaction was temperature but also that non-catalytic transesterification in ambient pressure (*i.e.,* 1 bar) could be achieved via providing thermal energy from an external heating source. Our previous work[16, 31, 32] reported that the heterogeneous reaction (*i.e.,* reaction between the gas phase of MeOH and the liquid phase of TGs) was established due to the low boiling point of MeOH (*i.e.,* T_b of MeOH = 65 ˚C). However, our previous work reported that derivatizing TGs into methyl ester was not occurred due to the short contact time between two different phases (*i.e.,* reaction between the gas phase of MeOH and the liquid phase of TGs). In order to resolve this in our previous work, we employed the porous materials, which was very effective. The porous material significantly increased the reaction time (*i.e.,* contact time) between two different phases by means of absorption and/or adsorption. The numerous pores provided the micro-reaction spaces that expedited the derivatization of TGs into FAME without using catalyst. The gas phase of MeOH acted like the mobile phase and the liquid phase of TGs acted like the stationary phase in the pores due to the low T_b of MeOH. These behaviors (*i.e.,* pseudo catalytic reaction) were very similar to the catalytic mechanisms. Note that catalytic phenomena are generally achieved by chemical or physical bonding of one of the chemical reagents, which then significantly enhances the frequencies of the collision among chemical reagents.

Therefore, our previous findings[16, 31, 32] can be applied for the analysis of the extracted lipid from the brain. In order to validate this, the derivatization of TGs into FAMEs was conducted with sunflower seed oil via the conventional (*i.e.,* NaOH used as catalyst) and the non-catalytic pathway. For the convenience sake, the conventional transesterification was illustrated as black colour and new technical derivatization was depicted as red colour. As indicated in Figure 1, the chromatogram was very similarly overlapped and their quantification was less than 2% error range. Thus, we can conclude that the introduced methodology in this study can be applicable for the lipid analysis.

Journal Name

COMMUNICATION

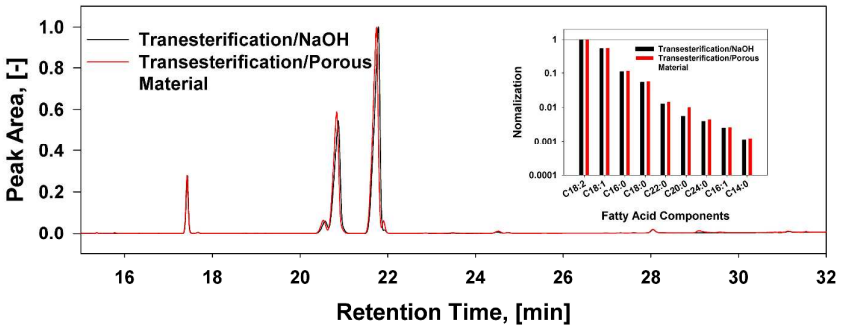

Figure 1. Representative chromatogram and normalization of quantified FAMEs based on C18:2-methyl ester (*i.e.,* linoleic acid methyl ester)at 400 ˚C

3.2. Lipid profiles of sectional bovine brain

In order to investigate the lipid profiles of the brain, the derivatizing technique should have extremely high tolerance of impurities including water and various extractives from the solvent extraction of bovine brain. Otherwise, the rigorous purification steps must be followed. In order to test tolerance against impurities, extracted lipid from bovine brain was transesterified in the presence of an acid/alkali catalyst. It was indeed confirmed that their conversions were nearly negligible (*i.e.,* less than ~1.5% conversion efficiency of FAMEs in the presence of alkali/acid catalyst).

Derivatization of extracted lipid from bovine brain into FAMEs in the presence of porous materials was successfully conducted even with a significant amount of impurities. For example, the water content of bovine brain is slightly higher than ~80 wt.%. Thus, extracted lipid from bovine brain would be a mixture of lipid, water, and extractives from the solvent extraction. One interesting observation was the derivatizing results in the presence of different pore sizes of silica (*i.e.,* 60 Å and 150 Å) were very similar, which could be an evidence for the non-catalytic transesterification reaction. For example, this observation suggested that the main driving force is temperature and that transforming the extracted lipid into FAMEs was not affected from the different pore sizes. The quantification and their comparison were illustrated and summarized in Figure 2 and Table 1.

The representative chromatogram in Figure 2(b) justified the stated high tolerance against impurities since extracted lipid without the purification step was transesterified in this work. For the sake of convenience, the peak identified as FAME was illustrated as a red colour. In Figure 2 (b), it is striking to find that the distribution of lipid compositions in each brain tissue was significantly different from each other. In order to compare the relative mass amounts of the different lipid profiles, the comparison in Figure 2 (c) was conducted based on the normalization. As illustrated in Figure 2 (c), the hexadecanoic acid methyl ester (C16:0) was used as the reference value for the normalization and the relative differences were depicted with a log scale (*i.e.,* Y-axis). Accordingly, significant differences were observed from each of all sectional brain samples. Table 2 summarized total quantities of lipids from each sectional brain sample of which relative mass normalization was exactly matching with the results in Figure 2 (c). Thus, this observation supports the compatibility of our approach, which also led to the total lipid content in the brain.

Although regional changes in brains have been identified in brain diseases, only a few studies have reported alternation of lipid profiles on region-specific alteration in patients' brains owing to the technical limitations (*i.e.,* the limited window of detectable lipid profiles, the large required amount of tissue, the time-consuming and labor intensive purification, and the relatively low reproducibility). Newly introduced derivatization techniques in this work, however, provide region-specific information on lipid profiles in Figure 2 (c) that will boost our understanding of the biochemical metabolisms, structures, and prevailed functions associated with brain diseases because the disease-related regional alternation usually accompanied with the changes of lipid profiles. Atrophy has been reported in the frontal cortex of patients with bipolar disorder. Cerebral atrophy and hippocampal atrophy have been known as a common feature of Alzheimer's disease and neuropsychiatric depression, respectively [8, 13, 33, 34]. Accordingly, the introduced technique is able to visualize the full spectrums of lipid components with a relatively small amount of brain tissue and

with a short analysis time via avoiding the rigorous purification steps.

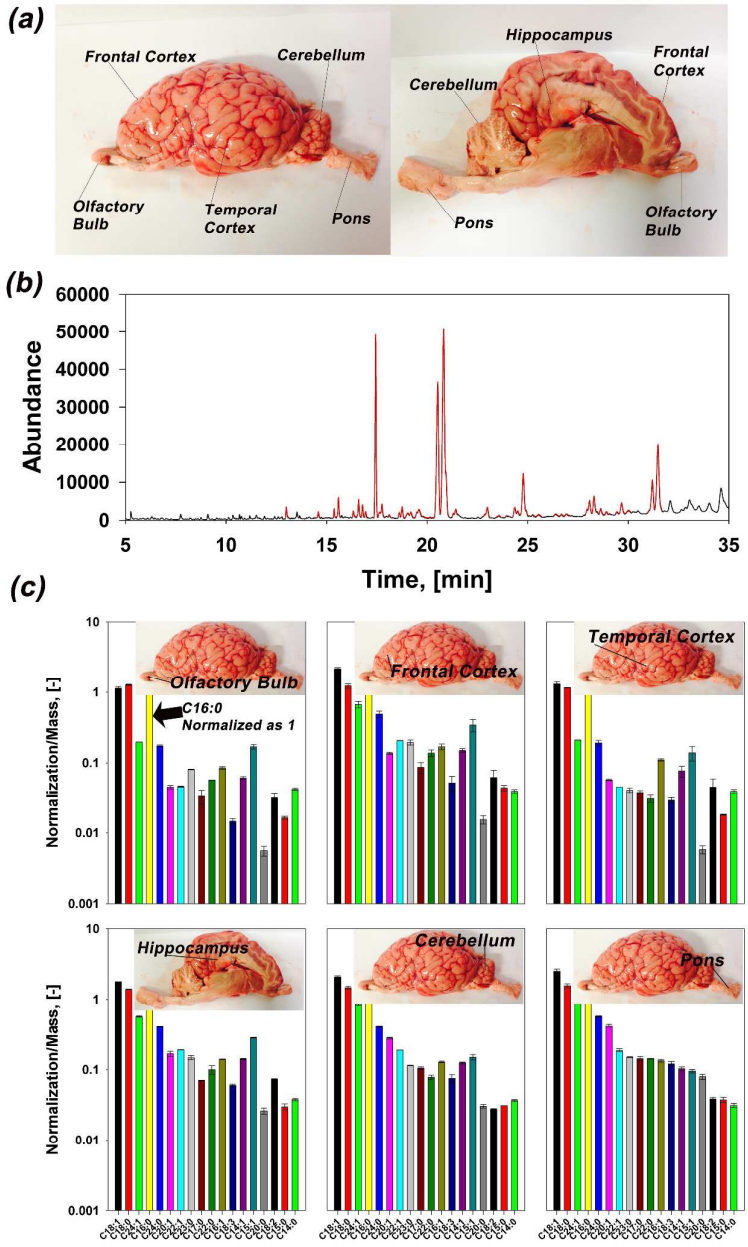

Figure 2. (a) Dissected bovine brain, (b) representative chromatogram of extracted lipid from pons at 400 ˚C, and (c) comparison of region-specific lipid composition

Journal Name

COMMUNICATION

Table 2. Summary of quantitative analysis of lipid samples from dissected bovine brain (all in mg unit with RSD (in %): N=3)

Order	Formula	Olfactory Bulb	Frontal Cortex	Temporal Cortex	Hippocampus	Cerebellum	Pons
1	C18:1	11.54 ± 5.63	16.89 ± 4.54	7.49 ± 7.95	17.27 ± 0.93	61.64 ± 3.77	127.91 ± 4.17
2	C18:0	12.97 ± 2.00	9.54 ± 6.78	6.66 ± 0.88	13.53 ± 1.05	43.74 ± 4.68	80.25 ± 3.77
3	C16:0	10.25 ± 3.74	7.83 ± 5.61	5.77 ± 7.27	9.7 ± 2.05	29.79 ± 2.34	51.04 ± 4.50
4	C24:1	2.01 ± 0.27	5.24 ± 10.61	1.21 ± 0.45	5.66 ± 2.87	25.73 ± 4.05	56.48 ± 0.74
5	C20:1	0.46 ± 5.79	1.06 ± 3.61	0.33 ± 2.72	1.63 ± 8.66	8.26 ± 3.31	21.76 ± 3.93
6	C24:0	1.77 ± 3.26	3.81 ± 10.28	1.1 ± 8.50	3.99 ± 1.86	12.14 ± 4.21	30.28 ± 1.37
7	C22:1	0.47 ± 1.65	1.61 ± 0.12	0.26 ±0.00	1.86 ± 0.06	5.61 ± 0.17	9.65 ± 2.93
8	C16:1	0.86 ± 3.9	1.32 ± 9.38	0.63 ± 3.51	1.37 ± 0.85	3.81 ± 2.59	6.94 ± 2.33
9	C22:0	0.58 ± 0.38	1.07 ± 9.98	0.18 ± 11.66	0.97 ± 13.41	2.32 ± 7.00	7.49 ± 0.47
10	C23:0	0.83 ± 0.84	1.52 ± 8.35	0.23 ± 7.23	1.44 ± 6.84	3.38 ± 0.85	7.85 ± 0.66
11	C17:0	0.34 ± 23.00	0.67 ± 17.04	0.22 ± 6.73	0.69 ± 0.43	3.12 ± 4.70	7.32 ± 3.81
12	C18:3	0.15 ± 7.72	0.41 ± 23.41	0.17 ± 8.71	0.58 ± 3.55	2.23 ± 13.36	6.18 ± 4.21
13	C14:1	0.62 ± 4.58	1.17 ± 5.75	0.44 ± 17.95	1.38 ± 1.97	3.7 ± 2.81	5.28 ± 3.08
14	C15:1	1.73 ± 7.02	2.66 ± 19.84	0.8 ± 23.20	2.75 ± 1.49	4.45 ± 8.66	4.91 ± 3.33
15	C20:0	0.06 ± 15.68	0.12 ± 13.07	0.03 ± 13.22	0.25 ± 9.76	0.9 ± 5.82	4.02 ± 5.25
16	C15:0	0.17 ± 5.04	0.34 ± 8.97	0.1 ± 1.65	0.29 ± 9.39	0.92 ± 0.16	1.89 ± 5.24
17	C18:2	0.32 ± 18.31	0.48 ± 26.75	0.26 ± 30.22	0.72 ± 0.84	0.83 ± 0.90	1.98 ± 2.93
18	C14:0	0.43 ± 3.61	0.31 ± 5.52	0.23 ± 6.50	0.37 ± 3.77	1.09 ± 2.22	1.6 ± 4.15
19	C22:2	0.08 ± 4.42	0.13 ± 21.35	0.08 ± 10.81	0.19 ± 2.47	0.23 ± 7.27	1.15 ± 1.05
-	Total	45.66 ± 3.27	56.2 ± 2.79	26.2 ± 4.96	64.7 ± 1.10	213.9 ± 3.09	254.09 ± 5.60

Journal Name

COMMUNICATION

Conclusions

A great deal of studies have been conducted to find a distinguished biomarker based on genome wide association studies, proteomics, to diagnose brain disease, and to be utilized as a potential target for screening a new drug. Among the numerous candidate markers from those investigations, the practical implementations have not been established due to individual differences[35]. Recent studies on lipidomics shed light on this situation, since metabolic imbalance in lipid profiles has more commonalities compared to genetic mutation or protein malfunction in brains of patients with neurodegenerative and neuropsychiatric diseases. In this regard, the qualitative and quantitative analysis of the lipid profiles of the brain has drawn a great deal of interest as a potential diagnostic marker of various brain diseases. Although the necessity of this research has been recognized from numerous studies, the discrepancies arising from the analytical limitations have significantly impeded practical applications. Accordingly, the technical advances achieved in this work will lead to an improved profiling of the lipid components based on the solvent extraction and non-catalytic fast methylation of sectional brain samples. The introduced novel method has an extremely high tolerance of impurities such as water and extractives from bovine brain and a wide detecting window of lipid profiles by minimizing the loss of lipid components during derivatizing processes; thus, it led to the enhancement of the resolution to visualize the whole spectrum of the lipid profiles in a sectional bovine brain. Furthermore, one of the major technical advantages achieved in this study is the qualitative and quantitative analysis of lipids from brain at trace quantities. Therefore, we expect that the proposed fast methylation technique will significantly contribute to a better understanding of the lipidomics and metabolic pathways by overcoming any unintended discrepancies associated with the traditional protocols for lipid composition analysis of brain. Considering the growing concerns over the cognitive and mood disorders in modern society, the introduced new technique in this study would help to reveal a valuable clue for elucidating metabolic markers to diagnose neurodegenerative and neuropsychiatric diseases. Furthermore, because of the many roles of lipids in cellular function, signal transduction and remodelling of cell membrane, a specific lipid component would be an attractive target to screen and validate the efficacy of new drugs for treating brain diseases.

Acknowledgements

This work was supported by the Basic Science Research Program through the National Research Foundation of Korea (NRF) and was funded by the Ministry of Education, Science, and Technology (NRF-2014R1A1A2055836).

Notes and references

1 S. Zhang, J. You, G. Zhou, C. Li and Y. Suo, *Talanta*, 2012, 98, 95-100.
2 H. S. Dhillon, T. Carbary, J. Dose, R. J. Dempsey and M. R. Prasad, *Brain Res*, 1995, 698, 100-106.
3 E. J. Murphy, *Prostaglandins Other Lipid Mediat*, 2010, 91, 63-67.
4 A. Della Corte, G. Chitarrini, I. M. Di Gangi, D. Masuero, E. Soini, F. Mattivi and U. Vrhovsek, *Talanta*, 2015, 140, 52-61.
5 E. Schwarz, S. Prabakaran, P. Whitfield, H. Major, F. M. Leweke, D. Koethe, P. McKenna and S. Bahn, *J Proteome Res*, 2008, 7, 4266-4277.
6 M. Vemuri, H. A. Kenna, P. W. Wang, T. A. Ketter and N. L. Rasgon, *J Psychiatr Res*, 2011, 45, 1036-1041.
7 R. B. Chan, T. G. Oliveira, E. P. Cortes, L. S. Honig, K. E. Duff, S. A. Small, M. R. Wenk, G. Shui and G. Di Paolo, *J Biol Chem*, 2012, 287, 2678-2688.
8 M. L. Bader Lange, G. Cenini, M. Piroddi, H. M. Abdul, R. Sultana, F. Galli, M. Memo and D. A. Butterfield, *Neurobiol Dis*, 2008, 29, 456-464.
9 M. Igarashi, K. Ma, F. Gao, H. W. Kim, D. Greenstein, S. I. Rapoport and J. S. Rao, *J Psychiatr Res*, 2010, 44, 177-182.
10 Y. Iwayama, E. Hattori, M. Maekawa, K. Yamada, T. Toyota, T. Ohnishi, Y. Iwata, K. J. Tsuchiya, G. Sugihara, M. Kikuchi, K. Hashimoto, M. Iyo, T. Inada, H. Kunugi, N. Ozaki, N. Iwata, S. Nanko, K. Iwamoto, Y. Okazaki, T. Kato and T. Yoshikawa, *Am J Med Genet B Neuropsychiatr Genet*, 2010, 153B, 484-493.
11 H. W. Kim, S. I. Rapoport and J. S. Rao, *Neurobiol Dis*, 2010, 37, 596-603.
12 M. Igarashi, K. Ma, F. Gao, H. W. Kim, S. I. Rapoport and J. S. Rao, *J Alzheimers Dis*, 2011, 24, 507-517.
13 B. N. Frey, J. A. Stanley, M. A. Nicoletti, J. P. Hatch and J. C. Soares, *Bipolar Disord*, 2008, 10, 849.
14 M. Kuloglu, B. Ustundag, M. Atmaca, H. Canatan, A. E. Tezcan and N. Cinkilinc, *Cell Biochem Funct*, 2002, 20, 171-175.
15 A. Versace, A. C. Andreazza, L. T. Young, J. C. Fournier, J. R. Almeida, R. S. Stiffler, J. C. Lockovich, H. A. Aslam, M. H. Pollock, H. Park, V. L. Nimgaonkar, D. J. Kupfer and M. L. Phillips, *Mol Psychiatry*, 2014, 19, 200-208.
16 E. E. Kwon, S. Kim, Y. J. Jeon and H. Yi, *Environmental Science & Technology*, 2012, 46, 10222-10228.
17 A. L. Bailey and S. Southon, *Analytical Chemistry*, 1998, 70, 415-419.
18 A. P. Birjandi, F. S. Mirnaghi, B. Bojko, M. W—àsowicz and J. Pawliszyn, *Analytical Chemistry*, 2014, 86, 12022-12029.
19 J. Deutsch, E. Grange, S. I. Rapoport and A. D. Purdon, *Anal Biochem*, 1994, 220, 321-323.
20 D. L. Gallaher and M. E. Johnson, *Analytical Chemistry*, 2000, 72, 2080-2086.
21 L. Hejazi, D. Ebrahimi, M. Guilhaus and D. B. Hibbert, *Analytical Chemistry*, 2009, 81, 1450-1458.

22 H. Ji, V. G. Voinov, M. L. Deinzer and D. F. Barofsky, *Analytical Chemistry*, 2007, 79, 1519-1522.
23 M. D. Leavell and J. A. Leary, *Analytical Chemistry*, 2006, 78, 5497-5503.
24 J. Li, Y. Yue, X. Hu and H. Zhong, *Analytical Chemistry*, 2009, 81, 5080-5087.
25 W. Reindl and T. R. Northen, *Analytical Chemistry*, 2010, 82, 3751-3755.
26 F. Robert-Peillard, E. Palacio-Barco, Y. Dudal, B. Coulomb and J.-L. Boudenne, *Analytical Chemistry*, 2009, 81, 3063-3070.
27 W.-C. Yang, J. Adamec and F. E. Regnier, *Analytical Chemistry*, 2007, 79, 5150-5157.
28 D. Kusdiana and S. Saka, *Fuel*, 2001, 80, 693-698.
29 M. Basselin, H. W. Kim, M. Chen, K. Ma, S. I. Rapoport, R. C. Murphy and S. E. Farias, *J Lipid Res*, 2010, 51, 1049-1056.
30 H. Blanchard, A. Y. Taha, Y. Cheon, H. W. Kim, J. Turk and S. I. Rapoport, *Neurochem Res*, 2014, 39, 1522-1532.
31 E. Kwon, H. Yi and Y. J. Jeon, *Environmental Science & Technology*, 2013, 47, 2817-2822.
32 E. E. Kwon, J. Seo and H. Yi, *Green Chemistry*, 2012, 14, 1799-1804.
33 R. M. Nitsch, J. K. Blusztajn, A. G. Pittas, B. E. Slack, J. H. Growdon and R. J. Wurtman, *Proc Natl Acad Sci U S A*, 1992, 89, 1671-1675.
34 J. D. Sluimer, H. Vrenken, M. A. Blankenstein, N. C. Fox, P. Scheltens, F. Barkhof and W. M. van der Flier, *Neurology*, 2008, 70, 1836-1841.
35 M. A. Slifer, E. R. Martin, P. G. Bronson, C. Browning-Large, P. M. Doraiswamy, K. A. Welsh-Bohmer, J. R. Gilbert, J. L. Haines and M. A. Pericak-Vance, *Am J Med Genet B Neuropsychiatr Genet*, 2006, 141B, 208-213.